

SEISMIC PERFORMANCE AND SHEAR RESISTING CAPACITY OF STEEL PLATE REINFORCED CONCRETE COUPLING BEAMS

G. Zhang¹ Z.Z. Zhao² and J.R. Qian³

¹ Postgraduate Student, ² Associate Professor, ³ Professor

Key Laboratory for Structural Engineering and Vibration of China Education Ministry in Department of Civil Engineering, Tsinghua University, Beijing, China

Email: civilzhang@gmail.com zzzhao@tsinghua.edu.cn qianjr@tsinghua.edu.cn

ABSTRACT :

Coupling beams of coupled shear wall system in seismic regions are required to have high load resisting capacity and excellent ductility and energy-dissipation capacity. To achieve this goal, the concept of steel plate reinforced concrete coupling beams (SPRCCB) is proposed. 6 SPRCCB specimens, 4 with a span-depth ratio of 1.5 and 2 with a span-depth ratio of 2.5, were tested under cyclic loading. Test results of the specimens are discussed. To further investigate the role of the steel plate in a SPRCCB, non-linear FE model based on one of the tested specimens was set up and verified. Based on this model, a parametric study was carried out to investigate the effect of the steel plate reinforcement ratio, the depth, thickness and depth-thickness ration of the steel plate on the shear resisting capacity of a SPRCCB. Some design recommendations were proposed based on the experimental and the analytical results.

KEYWORDS: Steel plate reinforced, Coupling beam, Experiment, FE analysis, Shear resisting capacity

1. INTRODUCTION

Steel plate reinforced concrete coupling beam (SPRCCB), in which steel plate is placed within the beam section and passes along the beam span, was proposed by Subedi (1989). According to the experimental results of Lam (2002), the performance of coupling beams was significantly improved and that the nominal shear strength of specimens was up to 10MPa. Although SPRCCBs have many advantages, researches on this kind of coupling beams are very limited and no designing guidelines were established on this kind of coupling beams. A research program has been carried out in Tsinghua University to evaluate the seismic performance of the SPRCCBs (Zhang, 2005). In this paper, some experimental and non-linear finite element study results on influence of the plate configuration such as the depth, width, depth-width ratio and reinforcement ratio etc., on shear resisting capacity of SPRCCB are reported.

2. EXPERIMENTAL STUDY

2.1. Test Specimens and Test Setup

Six coupling beam specimens (4 of them with a span-depth ratio of 1.5 and 2 with a span-depth ratio of 2.5) were tested (Zhang, 2005). Typical detailing of one specimen is shown in Figure 1. At each end of the specimen, there is a large rectangle panel cast integrally with the specimen, representing the wall block connected to the coupling beams. One steel plate was embedded along the beam span and was extended into wall blocks at both ends. A steel angle was welded at each end of the steel plate to ensure its anchorage in the wall blocks. To prevent the debonding and slip between the steel plate and surrounding concrete, two deformed bars were welded on each side of the steel plate. The thickness and clear span of the specimens were fixed at 150 mm and 750 mm respectively. Different span-depth ratios were obtained by varying the depth of the center beam. The specimens

with the same span-depth ratio have the same longitudinal and transverse reinforcement and the only variable was the steel plate, as shown in Table 1.

Table 1 Details of the specimens

Specimen	Depth (mm)	Span-depth ratio	Longitudinal bar	Stirrup	Steel plate $D \times t$ (mm ²)
CB15-1	500	1.5	2 Φ 16	2 Φ 8@100	220 x 6
CB15-2	500	1.5	2 Φ 16	2 Φ 8@100	420 x 3
CB15-3	500	1.5	2 Φ 16	2 Φ 8@100	350 x 6
CB15-4	500	1.5	2 Φ 16	2 Φ 8@100	200 x 10
CB25-1	300	2.5	4 Φ 16	2 Φ 8@120	220 x 3
CB25-2	300	2.5	4 Φ 16	2 Φ 8@120	220 x 6

The test setup was shown in Figure 2. The specimen was erected with beam longitudinal axis in vertical direction. One end of the specimen was fixed to the test floor through a rigid base beam and the other end was connected to an L-shaped steel loading frame. Shear load was applied to the specimen through the loading frame by an actuator, whose loading and support ends were pin-connected to the loading frame and the reaction wall respectively. The action line of the applied load passed through the center of the beam. A rotation restraining mechanism was installed to ensure equal end rotation of the specimen. Out-of-plane movements of the specimen were restrained by the roller guides. Self-weight of the loading frame was balanced by the dead weights.

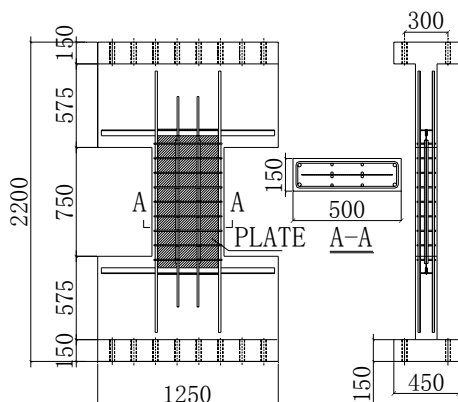


Figure 1 Dimensions of specimen CB15

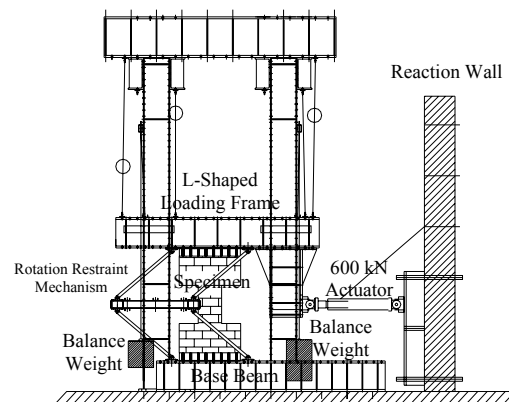


Figure 2 Test setup

2.2. Measurements and Loading Method

Displacements were measured using displacement transducers. Strains of the longitudinal bar, stirrups and steel plates were monitored using strain gauges. The crack development, failure sequence and failure modes were observed and recorded.

The specimens were tested under cyclic loading. The first two load cycles were under load control, with the maximum load being 50% and 100% of the predicted yield load respectively. The average top displacement in the two loading directions in the second cycle was taken as the yield displacement D_y . After that, test was under displacement control, with an increment of D_y . Each displacement level was repeated twice. The test stopped when the load resisting capacity of the specimen decreases to 70% of its peak load.

3. EXPERIMENT RESULTS

3.1. Crack Patterns and Failure Modes

The crack pattern of the specimens at the end of the test is shown in Figure 3. For specimen CB15-1, the inclined

shear cracks appeared after the longitude bars yielding. Stirrups yielded after the longitudinal bars yielding but before the peak load reached. After the peak load, the load resisting capacity decreased with yielding of the reinforcement and the crush of the concrete near the beam-wall interfaces. The steel plate did not yield at the end of test. The specimen was defined as flexural shear failure. Behavior of CB15-2 is similar to CB15-1. The longitudinal bars yielded first. The steel plate started to yield near one beam-wall interface and then yielded near the beam center. Stirrups yielded later than the steel plate but before the specimen reached its peak load. Typical load-strain curves of the longitudinal bars, stirrups and steel plate are shown in Figure 4. The specimen failed in flexural shear failure. Specimen CB15-4 failed in flexural shear failure as well. Stirrups in specimen CB15-3 yielded before the main longitudinal bars yielded. Existence of the steel plate prevents the development of the inclined shear cracks. More flexural cracks developed near the beam-wall interface and lead to crush of the concrete and wide opening of the flexural cracks near the beam-wall interface.

For CB25-1, stirrups yielded after the longitudinal bars yielded. The steel plate yielded when the specimen reached its peak load. Different from the former four specimens, some debonding cracks appeared along the main longitudinal bars after peak load. CB25-1 was defined shear failure. Behavior of CB25-2 was similar to CB25-1 but with higher load resisting capacity. CB25-2 failed in flexural-shear.

For coupling beams with small span-depth ratio (CB15 series), inclined shear cracks dominates which means shear force plays a major role in the crack and failure of the specimen. Because of the restraint of steel plate, the cracks at the centre of the specimen are not widely opened. From the cracking patterns, several detailing recommendations can be obtained. First, depth of the plate can not be too small compared with depth of the beam in order to provide good confinement of shear cracks and to facilitate the load transfer between the longitudinal bars and encased steel plate. Due to the relatively small plate height in specimens CB15-1 and CB15-4, they have similar funnel-shaped crack pattern and the concrete outside the plate restraint range severely cracked. In contrast, the shear crack in CB15-2 and CB15-3 which have a bigger steel plate depth is uniform. Second, stirrups are needed to prevent concrete spalling along the longitudinal bars. In CB25 series where the spacing of stirrups is relatively big, several longitudinal concrete spalling occurs till the end of the test (See Figure 3(e) and Figure 3(f)).

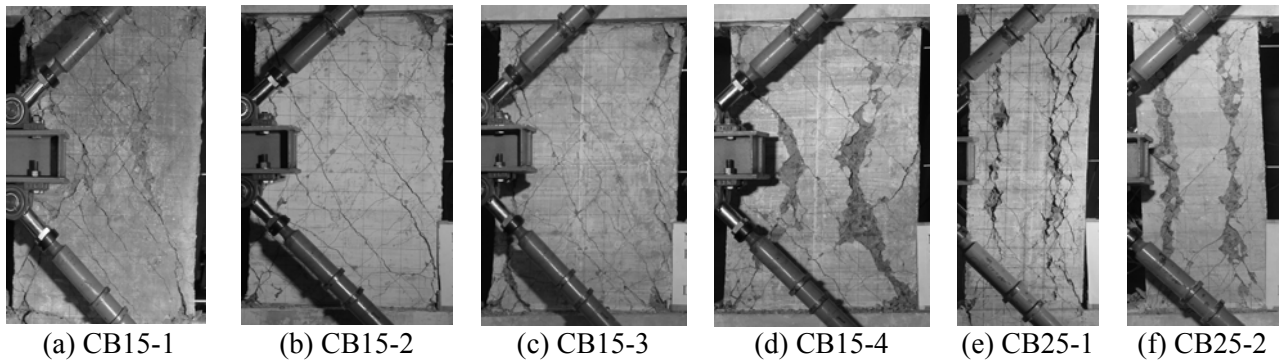


Figure 3 Typical crack pattern of the specimens after test

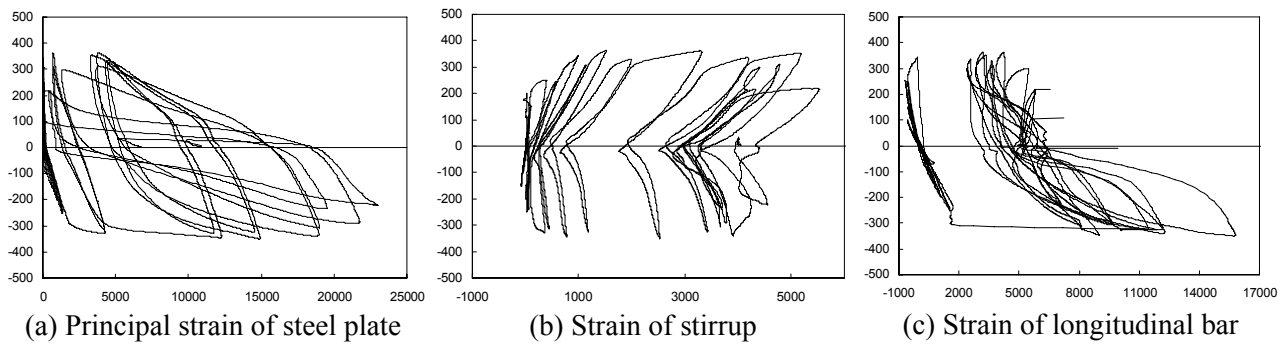


Figure 4 Load-strain curves of the specimens

3.2. Load Deflection Response

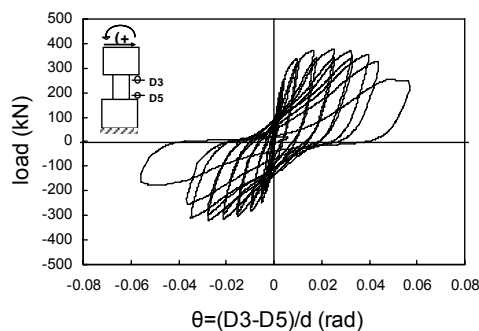
The typical load rotation curves of the specimens are shown in Figure 5. The results of the specimen tested by Zhao (2003) are also included for comparison. The load capacity and ductility of each specimen are listed in Table 2. V_y and V_u refer to the load when the longitudinal reinforcement yields and the peak load of the specimen respectively. The rotation of the specimen is calculated from $(D3-D5)/d$, where D3 and D5 are the reading of displacement transducer D3 and D5 shown in Figure 5 and d is the distance between them. θ_y , θ_u and θ_{u1} are beam rotation at yield load, peak load and ultimate stage respectively. The ultimate stage is defined as the state when the load resisting capacity dropped to 85% of the peak load. The ductility ratio is defined as the ratio of the beam rotation at a certain stage to the beam rotation at yield, as given in column 7 and 8 respectively.

Among CB15 series, CB15-3 and CB15-4 have the highest and lowest yield strength respectively, which may result from the depth of the steel plate in the specimen (see Table 1). CB15-1 and CB15-2 have similar steel plate reinforcement ratio and hence have similar shear resisting capacity. CB15-4 has a large steel plate but has the lowest shear resisting capacity. The reason is that the anchorage of the steel plate in the walls failed during the test and the steel plate did not reach its yield strength. To fully utilize the capacity of the steel plate, enough anchorage of the steel plate must be provided. The relative low load capacity of CB15-3 compared with that of CB15-1 may also be caused by similar reason.

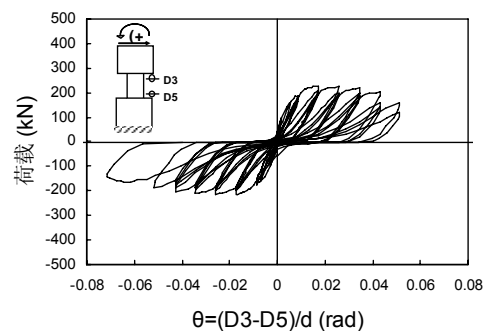
CB25-2 has a thicker steel plate than that of specimen CB25-1. Therefore, its load resisting capacity and energy dissipation capacity are much higher. Its yield load and peak load is increased by more than 20%. During post peak stage, yielding of the longitudinal bars and stirrups led to decreasing of load resisting capacity. However, the specimen with large plate section area has a stable load-deflection hysteretic curve. This proves that the minimum steel plate reinforcement ratio should be met to obtain desired performance. Comparing the hysteretic curves of the specimens with steel plate with those without steel plate, the existence of the steel plate in a coupling beam can not only increase its strength and energy dissipation capacity, but increase its stiffness and greatly reduce the pinching effect of the load-rotation curve.

Table 2 Load and deflection characteristic parameters of the specimens

Specimen	V_y (kN)	V_u (kN)	Rotation (10^{-3} rad)			Ductility ratio		Failure mode
			θ_y (rad)	θ_u (rad)	θ_{u1} (rad)	θ_u/θ_y	θ_{u1}/θ_y	
CB15-1	241	377	3.66	25.00	44.52	6.83	12.16	Flexural Shear
CB15-2	252	363	3.88	18.12	25.96	4.67	6.69	Flexural Shear
CB15-3	292	367	5.43	11.94	26.44	2.20	4.86	Flexural
CB15-4	223	340	3.76	12.25	31.38	3.26	8.35	Flexural Shear
CB25-1	156	198	7.71	16.23	26.81	2.10	3.48	Shear
CB25-2	191	254	6.56	14.91	29.54	2.27	4.50	Flexural Shear



(a) CB15-1



(b) CCB2 ($l/h=1.4$) (Zhao, 2003)

Figure 5 Load rotation curve of the specimens

3. PARAMETRIC STUDY

3.1. FE Modeling and Model Validation

A 2D nonlinear FE models are created using MSC. MARC (MSC, 2003). There are three types of elements in the model. Concrete and the steel plate are modeled using 4-node iso-parametric element and the longitudinal bars and stirrups are modeled using 4 node rebar element. It was assumed that the concrete and the steel (including the reinforced bars and steel plate) work perfectly together and no slip occurs. One end of the model is fixed and the horizontal (the direction that is perpendicular to the axial direction of the coupling beam) degree of freedoms on the other end of the model are coupled to restrict the end rotation at the loading end. Figure 6 shows an overview of the FE mesh results of the model.

The constitutive relationship of the concrete follows the model proposed by Guo (1999) and was simulated using multi-linear approximation. The stress-strain relationship of concrete is shown in Figure 7(a) and the value of parameters is listed in Table 2(a). Smearred crack model is adopted to deal concrete cracking. The adopted stress-strain relationship and strength parameters of steel are shown in Figure 8(b) and Table 2(b) respectively.

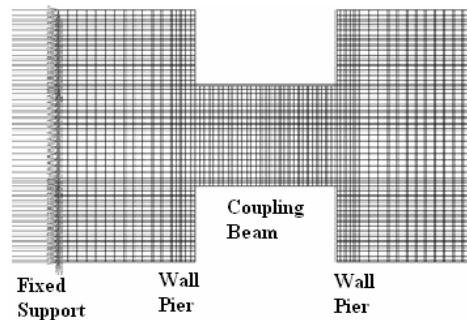


Figure 6 Finite Element Model of Coupling Beam

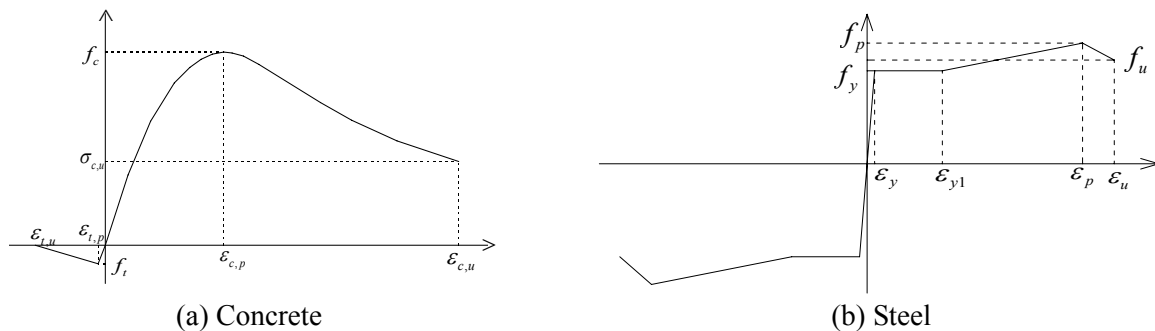


Figure 7 Material Properties

Table 3(a) Material parameters of the concrete

$\epsilon_{c,p}$	$\epsilon_{l,p}$	$\epsilon_{c,u}$	$\epsilon_{l,u}$	f_i	$\sigma_{c,u}$
0.00250	-0.000130	0.00742	-0.00146	$-0.1 f_c$	$0.434 f_c$

Table 3(b) Material parameters of the steel plate and the reinforcing bars

ϵ_y	ϵ_{y1}	ϵ_p	ϵ_u	f_p	f_u
f_y/E_s	0.02	0.15	0.17	$1.4 f_y$	$1.1 f_y$

In order to verify the reliability of the FE model, the predicted results are compared with the experimental results for CB15-2. Figure 8 and Figure 9 shows the strain distribution at beam-wall interface and strains along the

longitudinal reinforcement under different ductility level. It can be seen that the experimental and FE results are quite consistent. The “tension lag” (the zero strain point moves towards the compression zone after the appearance of the shear crack.) can also be seen from Figure 15. The over-estimation of strain in the FE model may result from the assumption that there is no bond-slip between the steel bar and the around concrete. At large displacement level (such as $\mu=2$), the width of the concrete cracks is big and so the FE analysis gives a big strain value, while in fact, due to the existence of local bond-slip, the measured strain on the longitudinal bar is smaller than the strain induced by the wide crack of concrete. The predicted load-rotation curve fits with the envelope of the experimental hysteric curve quite well even though the FE analysis gives a higher prediction of load resisting capacity and stiffness. Generally, FE method can give a quite accurate prediction of the experimental results.

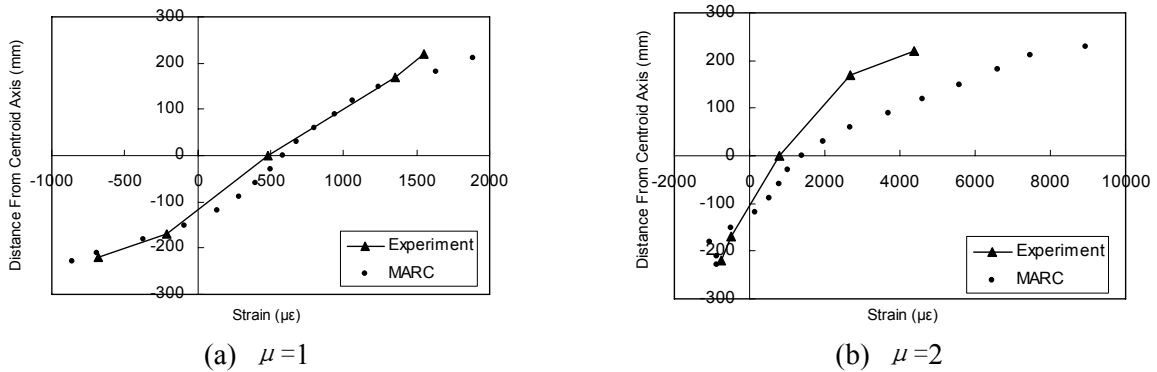


Figure 8 Strain Distribution at the Wall-Beam Interface

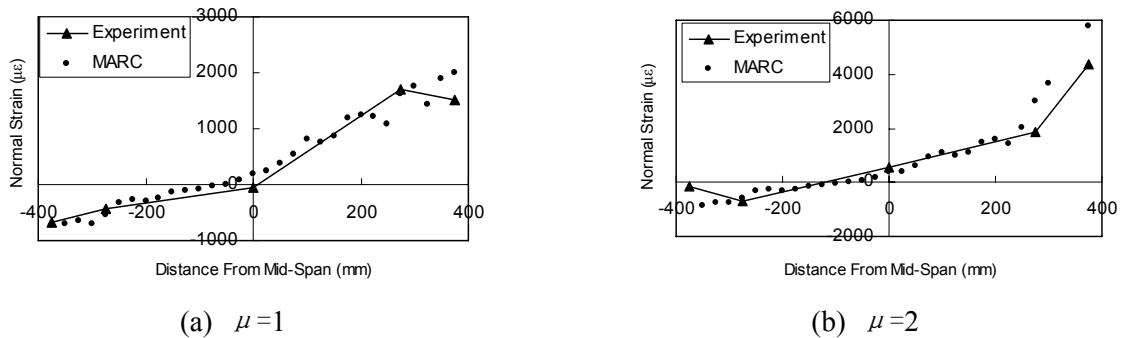


Figure 9 Strain Distribution along Beam Axis

3.2. Parametric Study

In order to find the effect of plate depth and thickness, etc. on shear resisting capacity of a coupling beam, parameter studies were carried out. Table 4 lists the material properties of the model, in which f_c is the concrete compressive strength; f_y , f_p and f_{yv} are the yield strength of the longitudinal bars, the plate and the stirrups respectively; ρ_s is the longitude reinforcement ratio and ρ_{sv} is the shear reinforcement ratio. Results of the model with different parameters are shown in Table 5. For comparing, the shear resisting capacity is expressed in terms of peak nominal shear stress τ_p . Figure 10 shows the influence of plate reinforcement ratio on the value of τ_p . It can be seen from the figure that the shear resisting capacity of a coupling beam increased linearly with the plate reinforcement ratio.

The effect of the plate thickness is given in Figure 11, where the horizontal axis is the plate thickness and the vertical axis is the shear resisting capacity. From experimental results, it was found that the crack pattern of the beam with a large steel plate height is different from the one with a small plate height. In order to consider this, two different plate heights are considered. The rectangle dot refers to the specimens with a plate depth of 420mm and the hollow dot represents the one with a plate depth of 180mm. It is clear that the shear resisting capacity increases as the plate thickness increases. But the shear strength of a specimen with a deeper plate increases

faster than that of a specimen with a lower plate. This is because the concrete that is not in the range of steel plate is prone to crack under low load, which makes the load transfer between the longitudinal bars and the plate difficult, see Figure 12. So, the plate can not be too small in order to be effective in shear resisting. Based on the experimental results, the depth of plate should not be less than the 70% of the beam depth.

Table 4. Invariable Parameters in the analysis

f_c (MPa)	f_y (MPa)	f_{yv} (MPa)	f_p (MPa)	ρ_s (%)	ρ_{sv} (%)
34.8	380	308	345	2.84	0.67

Table 5 Parametric Analysis Results

Model	Depth (mm)	Thickness (mm)	Plate Area (mm ²)	Steel Plate Reinforcement Ratio (%)	Load Capacity (kN)	$\tau_p=V/bh_0$ (MPa)
1	180	1.0	180	0.26	442.04	6.27
2	180	3.0	540	0.76	488.94	6.94
3	420	1.5	630	0.89	623.77	8.85
4	180	5.0	900	1.28	512.94	7.28
5	300	3.0	900	1.26	569.96	8.08
6	180	6.0	1080	1.53	587.20	8.33
7	360	3.0	1080	1.53	637.36	9.04
8	180	7.0	1260	1.79	528.91	7.50
9	300	4.2	1260	1.79	609.77	8.65
10	360	3.5	1260	1.79	690.51	9.79
11	420	3.0	1260	1.79	784.95	11.13
12	300	6.0	1800	2.55	744.26	10.56
13	420	4.5	1890	2.68	934.29	13.25
14	360	6.0	2160	3.06	845.29	11.99
15	180	14.0	2520	3.57	646.70	9.17
16	300	8.4	2520	3.57	782.49	11.10
17	360	7.0	2520	3.57	897.28	12.73
18	420	6.0	2520	3.57	1030.45	14.62

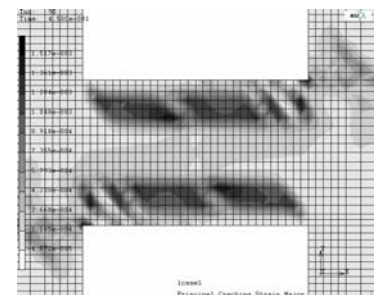
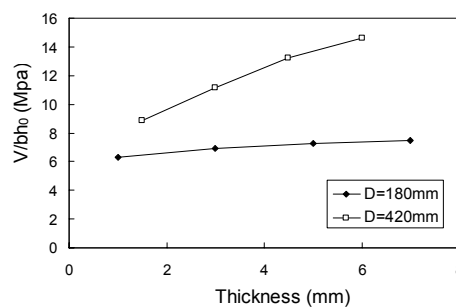
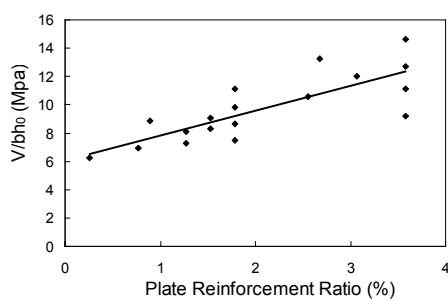


Figure 10 Effect of plate reinforcement ratio Figure 11 Effect of plate thickness Figure 12 Crack pattern

Figure 13 presents the effect of the plate depth on beam shear resisting capacity. The shear resisting capacity of the beam increases with the plate depth increase, but not linearly. The increment becomes larger when the steel plate becomes deeper. Figure 14 shows the relationship between the depth/thickness ratio and the shear resisting capacity of a beam under different plate reinforcement ratio. The shear resisting capacity increases linearly as the value of D/t become bigger. It is also clear that for a beam with a higher plate reinforcement ratio, its shear resisting capacity increase much faster than that with a small plate reinforcement ratio. This means that the minimum plate reinforcement ratio should be limited in order to make the steel plate to be effective. Based on our study, it is recommended that the steel plate reinforcement ratio should not less than 1.8%.

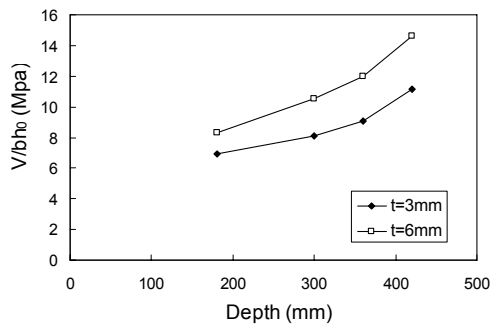


Figure 13 Influence of Plate Depth

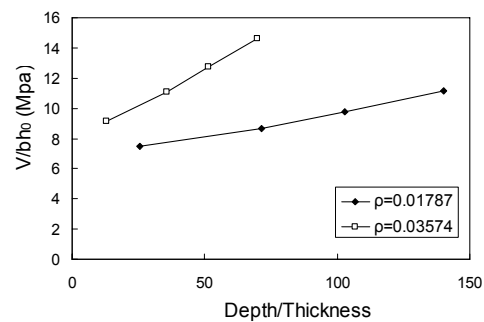


Figure 14 Influence of Depth/Thickness Ratio

4. CONCLUSIONS

Based on the non-linear finite element study on SPRCCB specimens, the following conclusions are drawn:

- 1) The shear strength of SPRCCB increases with the steel plate reinforcement ratio.
- 2) Increasing the thickness and depth of the steel plate will increase the shear strength of a SPRCCB, but the increment of shear resisting capacity will be more obvious when the depth of steel plate is larger. The depth of steel plate should be limited and a minimum depth of 70% of the beam depth is suggested based on our experimental results
- 3) Two SPRCCB specimens with same ratio of the steel plate reinforcement, the shear resisting capacity of the one with large depth-thickness ratio will be larger. The effect of depth-thickness ratio is more obvious in the SPRCCBs with a bigger steel plate reinforcement ratio. A minimum steel plate reinforcement ratio of 1.8% is recommended based on experimental and analytical results.

REFERENCES

- Guo Z.H. (1993). Principles of Reinforced Concrete” (in Chinese), Tsinghua University Press, Beijing, China.
- Lam W.Y. (2002). Experimental study on embedded steel plate composite coupling beams, M.S. Thesis, The University of Hong Kong.
- MSC. Software Corporation. MSC.Marc: Theory, User Information and Element Library, Version 2005. U.S.A. MSC.Software Corporation, 2005.
- Subedi N.K. (1989). Reinforced concrete beams with plate reinforcement for shear, *Proceedings of the Institution of Civil Engineers, Structural Engineering*, **87(Part2)**, 377-399.
- Zhang G. (2005). Experimental Study on Seismic Behavior of Steel Plate Reinforced Concrete Coupling Beams, M. Phil. Thesis, Tsinghua University.
- Zhao Z.Z. and Kwan, A.K.H. (2003). Nonlinear behavior of deep reinforced concrete coupling beams, *Structural Engineering and Mechanics* **15:2**, 181-198.